

Article

Spatiotemporal Patterns and Characteristics of PM_{2.5} Pollution in the Yellow River Golden Triangle Demonstration Area

Ning Jin ¹, Liang He ^{2,*}, Haixia Jia ¹, Mingxing Qin ³, Dongyan Zhang ^{4,*} , Cheng Wang ¹, Xiaojian Li ¹ and Yanlin Li ¹

¹ Department of Resources and Environmental Engineering, Shanxi Institute of Energy, Jinzhong 030600, China; jinn.13b@igsnr.ac.cn (N.J.)

² National Meteorological Centre, Beijing 100081, China

³ College of Resources and Environment, Shanxi Agricultural University, Taigu 030800, China; qmx758@sxau.edu.cn

⁴ College of Mechanical and Electronic Engineering, Northwest A&F University, Yangling 712100, China

* Correspondence: heliang@cma.gov.cn (L.H.); zhangdy@ahu.edu.cn (D.Z.)

Abstract: Improving air quality in the Yellow River Golden Triangle Demonstration Area (YRGTD) is an important practice for ecological protection and high-quality development in the Yellow River Basin. Preventing and controlling PM_{2.5} pollution in this region will require a scientific understanding of the spatiotemporal patterns and characteristics of PM_{2.5} pollution. PM_{2.5} data from different sources were combined in this study (the annual average of PM_{2.5} concentrations were obtained from the Atmospheric Composition Analysis Group of Dalhousie University, and the daily PM_{2.5} concentration data were obtained from the China National Environmental Monitoring Centre). Then, the temporal variation of PM_{2.5} concentrations at annual, seasonal, and monthly scales, the spatial variation of PM_{2.5} concentrations, and the variation of PM_{2.5} pollution classes were analyzed. Results showed that: (1) at the annual scale, the PM_{2.5} concentrations showed a decreasing trend from 2000 to 2021 in the study area. The variation of PM_{2.5} concentrations were divided into two different stages. (2) At the seasonal scale, high PM_{2.5} concentrations occurred mainly in winter, low PM_{2.5} concentrations occurred in summer. At the monthly scale, PM_{2.5} concentrations showed a U-shaped variation pattern from January to December each year. (3) The hotspot analysis of the PM_{2.5} concentrations in the study area showed a cyclical variation pattern. (4) The PM_{2.5} concentrations exhibited a spatial pattern of high values in the central and low values in the northern and southern parts of YRGTD. (5) The number of days for different PM_{2.5} pollution classes from 2015 to 2021 followed the order of Good > Excellent > Light pollution > Moderate pollution > Heavy pollution > Severe pollution in YRGTD. The results of this study have great theoretical and practical significance because they reveal the spatiotemporal patterns and pollution characteristics of PM_{2.5} and will lead to the development of scientifically based measures to reasonably prevent and control pollution in YRGTD.

Keywords: PM_{2.5} concentration; temporal variation; spatial variation; pollution level



Citation: Jin, N.; He, L.; Jia, H.; Qin, M.; Zhang, D.; Wang, C.; Li, X.; Li, Y. Spatiotemporal Patterns and Characteristics of PM_{2.5} Pollution in the Yellow River Golden Triangle Demonstration Area. *Atmosphere* **2023**, *14*, 733. <https://doi.org/10.3390/atmos14040733>

Academic Editors: Cheng Li, Fan Yang, Qitao Xiao and Yao Gao

Received: 9 March 2023

Revised: 11 April 2023

Accepted: 13 April 2023

Published: 19 April 2023



Copyright: © 2023 by the authors. Licensee MDPI, Basel, Switzerland. This article is an open access article distributed under the terms and conditions of the Creative Commons Attribution (CC BY) license (<https://creativecommons.org/licenses/by/4.0/>).

1. Introduction

In recent years, with accelerated urbanization occurring in China, the rapid increasing in urban population and energy consumption has led to many ecological and environmental problems [1]. As one of the world's largest developing countries and fastest-growing economies, the problem of urban air pollution that accompanies rapid economic development has received increasing attention from the government and society in China. PM_{2.5} is an air pollutant that is also the primary pollutant affecting air quality in most cities [2–6]. PM_{2.5} usually comes from vehicle exhaust, industrial production, and coal burning in winter. The dispersion and accumulation of PM_{2.5} are influenced by different meteorological conditions and topographic factors that ultimately induce different regional pollution characteristics [7,8]. Massive emissions of PM_{2.5} reduce air quality, affect atmospheric visibility

and traffic safety, and damage ecosystems and public health [9,10]. Energy consumption in China has remained high for a long time and has induced a series of environmental problems, such as air pollution [11]. In September 2020, China made a commitment to “carbon neutrality and emission peak” to the international community. Then, in late September 2021, China officially announced that it would stop developing new coal power projects overseas. These overseas energy investments are now shifting from coal to clean energy, thus lending fresh impetus to the global net-zero emissions transition and helping to reduce particulate matter emissions to improve atmospheric conditions. The report to the 20th National Congress of the Communist Party of China states that the Chinese government will continue to control pollution; make further efforts to keep skies blue, waters clear, and lands clean, and basically eliminate serious air pollution. Therefore, it is of great practical significance to effectively prevent and control PM_{2.5} pollution based on the results of studies regarding the spatiotemporal variations of PM_{2.5}.

Currently, studies on PM_{2.5} have mainly focused on the following aspects: (1) the research objectives are mainly directed at the spatiotemporal distribution of PM_{2.5}, chemical component characteristics and source analysis, pollutant propagation and dispersion, the relationship between PM_{2.5} and natural conditions as well as socioeconomic activities, and impacts on human health [12,13]. (2) The research scales cover national, provincial, regional, and city scales [14–16]. (3) Many regional studies are focused on economically developed regions, such as the Beijing-Tianjin-Hebei province, the Yangtze River Delta, and the Pearl River Delta, and relatively few studies are focused on the less developed regions such as central and western China [17]. (4) The data used come from ground observations and satellite remote sensing monitoring [18]. Studies have been conducted on the spatiotemporal patterns of PM_{2.5} at national, regional, provincial, and city scales using ground data [19]. The advantages of ground data are accuracy, reliability, and continuity. Generally, these data have high temporal resolution and can reveal PM_{2.5} variation characteristics at different time scales such as hourly, daily, monthly, quarterly, and annual [20–22]. The primary disadvantage of ground data is the limited number of ground PM_{2.5} monitoring stations in a region that makes it difficult to fully reflect the continuous spatial variations of PM_{2.5} using only these data [23]. A good correlation exists between aerosol optical depth (AOD) derived from satellite remote sensing data and ground-observed particulate matter concentration. The lack of spatial representation for ground observations can be effectively compensated for by using PM_{2.5} data estimated by AOD data [24,25]. The shortcomings in estimating PM_{2.5} data using satellite remote sensing data are as follows. Firstly, optical satellite remote sensing data are often affected by weather conditions, especially cloud cover [26]. Secondly, satellite remote sensing data are instantaneous values, so only instantaneous PM_{2.5} concentrations can be estimated. Thirdly, due to the scalability of the PM_{2.5} concentration estimation model, the model parameters need to be adjusted when applying these models to different regions [27]. Fourthly, PM_{2.5} data estimated using satellite remote sensing data cannot reflect specific types of particulate matter, chemical components, and chemical characteristics [28]. Therefore, combining different sources of PM_{2.5} data will be helpful for improving the reliability of PM_{2.5} analysis results.

At present, studies regarding regional PM_{2.5} pollution in China are mainly focused on the economically developed regions, with less attention being given to less developed regions. In 2019, Chinese President Xi Jinping declared the ecological protection and high-quality development of the Yellow River Basin as a major national strategy. The Yellow River Golden Triangle Demonstration Area (YRGTD) is located at the junction of Shanxi, Shaanxi, and Henan provinces. This region is an inter-provincial intersection area in the combined belt of the central and western regions of China. Due to the influence of topographical factors, meteorological conditions, coal combustion, industrial pollution, and vehicle emissions, the YRGTD has long been one of the most seriously air-polluted areas in China. There is a trend for the air pollution to evolve from single city to regional areas, and this region is a key air pollution control area in China. Smog pollution has complex spatial correlation and spillover effects, and there is a complex interdependence and strong spatial interaction between different regions. Achieving the dual goals of high-

quality urbanization development and ecological civilization construction is important in YRGTD. There is an urgent need to determine the spatiotemporal characteristics of $PM_{2.5}$ pollution and to clarify the relationship between different development stages of urbanization and $PM_{2.5}$ concentration in order to propose effective prevention and control measures in YRGTD. Many studies have focused on the analysis of spatiotemporal variation of $PM_{2.5}$ concentrations, while few studies have been conducted on the statistical analysis of the $PM_{2.5}$ pollution processes. Clarifying the variation characteristics, classification, and occurrence mechanism of the $PM_{2.5}$ pollution processes in YRGTD will have great practical significance for joint cross-regional air pollution prevention and control and for reducing the harm caused by $PM_{2.5}$ pollution.

This study was conducted for YRGTD to determine the spatiotemporal variation characteristics of $PM_{2.5}$ concentrations and pollution levels on annual, seasonal, and monthly scales. In order to achieve this goal, geostatistical and spatial data analysis methods were used based on the combining of $PM_{2.5}$ data derived from ground station monitoring and satellite remote sensing estimation. Then, the fluctuation and geographic variation characteristics of $PM_{2.5}$ spatiotemporal patterns in YRGTD were revealed. The results of this study are expected to provide theoretical references and a scientific basis for the joint prevention and control of $PM_{2.5}$ pollution so that there will be a reduction in exogenous $PM_{2.5}$ pollution in the urban clusters and urban agglomerations, with the ultimate result being the ecological protection and high-quality development of YRGTD.

2. Materials and Methods

2.1. Study Area

The location of YRGTD is shown in Figure 1 ($33^{\circ}31' E-36^{\circ}57' E$, $108^{\circ}58' N-112^{\circ}34' N$), including four prefecture-level cities (Linfen, Yuncheng, Weinan, and Sanmenxia) in three provinces (Shanxi, Shaanxi, and Henan), with a total of 47 counties. The YRGTD is located at the junction of the central and western parts of China, and acts as a bridge between the east and the west, and the north and the south of China. The area of this region is $58,010 \text{ km}^2$ (0.604% of China's land area). The total population is 15.3146 million (1.084% of China's total population). The regional GDP is 7.63235 hundred billion RMB (0.667% of China's total GDP) (China Statistical Yearbook 2021).

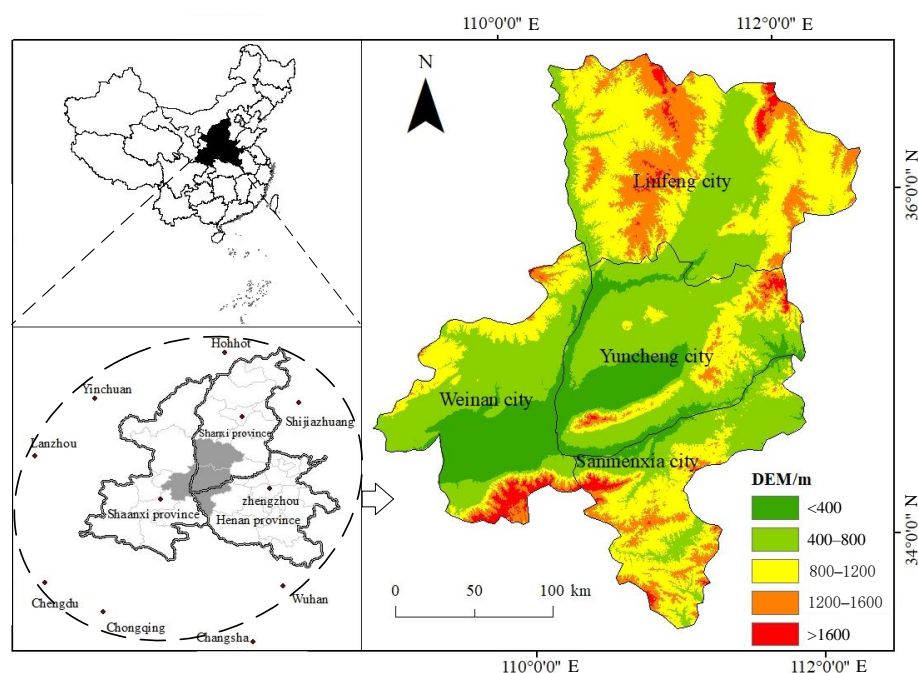


Figure 1. Location of the Yellow River Golden Triangle Demonstration Area, China.

2.2. Data

In 2012, the Ministry of Environmental Protection of China officially declared PM_{2.5} concentration as one of the air quality monitoring indices and established corresponding evaluation standards. Real-time monitoring data from the national automatic air quality monitoring stations were first officially released to the public in 2013. Daily PM_{2.5} concentration data used in this study were obtained from the real-time national urban air quality release platform of the China National Environmental Monitoring Centre. The daily PM_{2.5} concentration data covers a period from 1 January 2015 to 28 February 2022. The average PM_{2.5} for the 2021 winter were calculated with data from December 2021 to February 2022.

Currently, remote sensing data and machine learning methods have been widely used to estimate and analyze the spatiotemporal variation of PM_{2.5} concentrations. Many organizations have published global and regional PM_{2.5} concentration raster datasets. In order to determine the long-term spatiotemporal evolution characteristics of PM_{2.5}, a long time series of county-level PM_{2.5} data from 2000 to 2018 was used in this study, available from the Atmospheric Composition Analysis Group of Dalhousie University. The PM_{2.5} data derived from the Atmospheric Composition Analysis Group of Dalhousie University have been widely used in many studies. Van et al. (2016) calibrated and verified the reliability of this data using the PM_{2.5} data from global, ground-based observations, with an R² value that reached 0.817 between the two data [29]. Therefore, the reliability of this data was not validated in this study.

2.3. PM_{2.5} Pollution Levels

According to the Ambient Air Quality Standards (GB3095-2012) of the Ministry of Environmental Protection of China, the daily average PM_{2.5} concentration pollution levels were divided into six classes: Excellent (0–35 µg/m³), Good (35–75 µg/m³), Light pollution (75–115 µg/m³), Moderate pollution (115–150 µg/m³), Heavy pollution (150–250 µg/m³), and Severe pollution (>250 µg/m³).

2.4. Data Processing Methods

2.4.1. Trend Analysis

The slope reflecting the trend of the PM_{2.5} time series data was obtained using the one-dimensional linear regression method [30]. A positive slope value indicated an increasing trend of PM_{2.5} concentration, while a negative value reflected a decreasing trend. The spatial distribution of PM_{2.5} variation trends in YRGTD was plotted based on the trend analysis for each county. Then, the multi-year variation trends of PM_{2.5} concentration and the regions where PM_{2.5} increased or decreased over the years were revealed.

The PM_{2.5} concentrations data were analyzed using Mann-Kendall analysis method and the Z statistic values were calculated. When Z statistic value > 0, it indicates the PM_{2.5} concentrations data have an increasing trend; while when Z statistic value < 0, it indicates the PM_{2.5} concentrations data have a decreasing trend. When the value of |Z| is greater than or equal to 1.64, 1.96, or 2.58, it means the PM_{2.5} concentrations data pass the significance test at 90%, 95%, and 99% confidence level, respectively.

2.4.2. Statistics of PM_{2.5} Pollution Process

Spatial autocorrelation refers to the geographical element distributed in different spatial locations, one of its attribute values has a statistical correlation. Generally, the closer the distance, the greater the correlation. Spatial autocorrelation is an important indicator to test whether the attribute value of an element is correlated with the attribute value of its spatial neighboring points. The positive correlation indicates that the attribute value change of a unit has the same variation trend with its spatial neighboring units. This reflects the agglomeration of spatial phenomena, while it is the opposite for the negative correlation [31–33].

Regions with statistically significant PM_{2.5} concentrations were identified using the hotspot analysis method based on the spatiotemporal analysis of PM_{2.5} data. The hotspot

analysis function in the GIS software was used to get the calculation results, and then the z-score values were obtained. For statistically significant positive z-score values, the higher the z-score value, the tighter the aggregation of high PM_{2.5} concentrations. Whereas for statistically significant negative z-score values, the lower the z-score value, the tighter the aggregation of low PM_{2.5} concentrations.

3. Results

3.1. Temporal Variation Characteristics of PM_{2.5} Concentrations in YRGTD

3.1.1. Annual Variation Characteristics

The annual average PM_{2.5} concentrations from 2000 to 2021 showed a characteristic of increasing first and then decreasing in YRGTD (the highest value occurred in 2011). The PM_{2.5} concentrations showed an increasing trend (from 48 µg/m³ to 85 µg/m³) from 2000 to 2011 and an obvious decreasing trend from 2011 to 2021 (from 85 µg/m³ to 45 µg/m³) (Figure 2). The year of 2011 was an important inflection point for the variation of annual average PM_{2.5} concentrations in YRGTD. This clear and sustained reduction in PM_{2.5} concentrations was related to national ecological civilization construction efforts, industrial structure upgrading and adjustments, and energy use efficiency improvements that reduced the particulate matter emissions to a certain extent. The PM_{2.5} concentrations in 2021 were basically comparable to the concentrations in 2000, indicating the PM_{2.5} pollution during 2011–2021 had been significantly controlled.

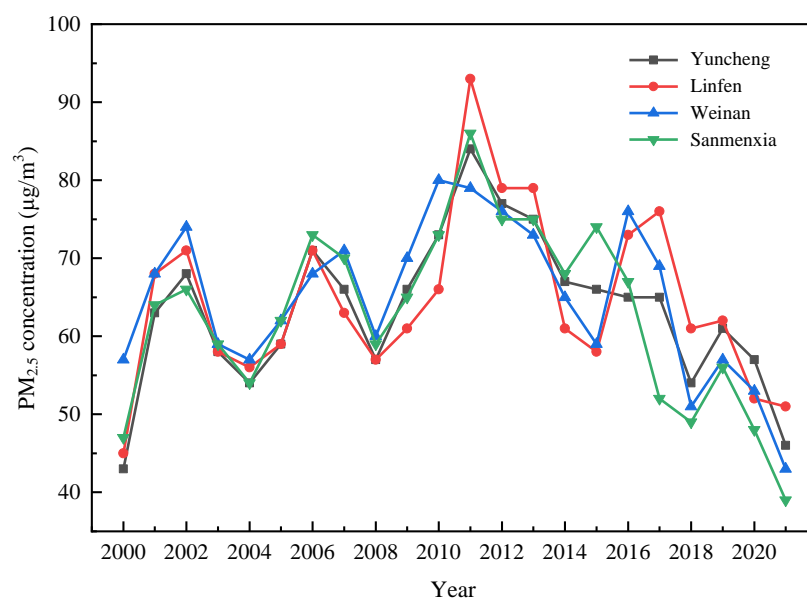


Figure 2. Average PM_{2.5} concentrations from 2000 to 2021 for four cities in the Yellow River Golden Triangle Demonstration Area, China.

3.1.2. Seasonal Variation Characteristics

Seasonal variation of PM_{2.5} concentrations showed a characteristic of high values in winter, low values in summer, and transitional values in spring and autumn in YRGTD. The seasonal PM_{2.5} concentrations in this region during 2015–2021 had been effectively controlled. The PM_{2.5} concentrations in spring, summer, autumn, and winter showed decreasing trends of $-3.3095/\text{yr}$, $-3.4762/\text{yr}$, $-3.0119/\text{yr}$, and $-6.8839/\text{yr}$, respectively. The Z statistic values of spring and, summer, autumn, and winter were -2.403 , -2.403 , -1.2015 , and -1.5019 , respectively. The Z statistic value of spring and summer passed the significance test of 95%, 95%. The decreasing degrees of PM_{2.5} concentrations were basically comparable in spring, summer, and autumn, while the PM_{2.5} concentrations decreased to a greater degree in winter than in the other three seasons (Figure 3). The variations of PM_{2.5} concentrations in YRGTD were closely related to the activities of burning coal for

heating in winter, industrial pollution, vehicle emissions, and the local topographic and climatic conditions. The $PM_{2.5}$ concentrations in this region showed a significant decreasing trend in winter after 2016 that may be closely related to the national promotion of urban heating system renovation, which included a widespread reduction in the use of raw coal for heating, instead using natural gas.

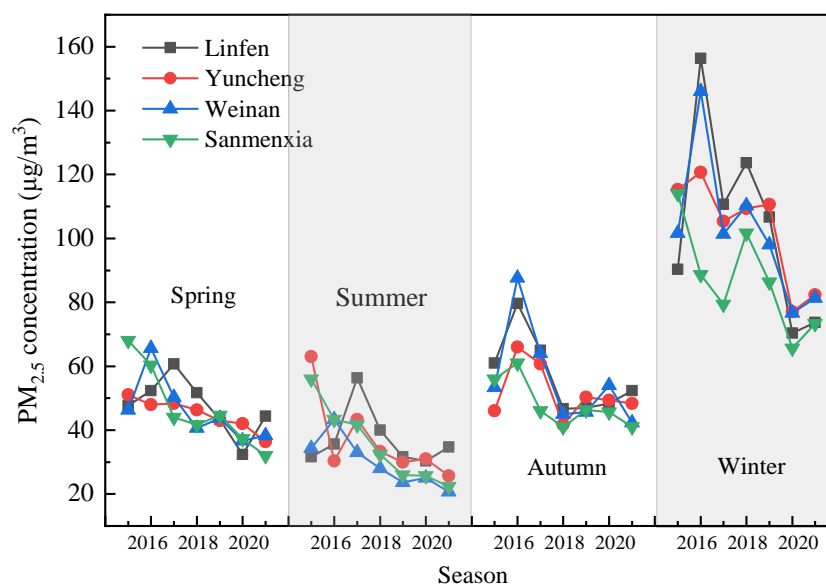


Figure 3. Seasonal variation of $PM_{2.5}$ concentrations in the Yellow River Golden Triangle Demonstration Area, China.

3.1.3. Monthly Variation Characteristics

The changing trend of monthly average $PM_{2.5}$ concentration values from January to December were basically the same (U-shaped trend) for all four cities in YRGTDA (Figure 4). The $PM_{2.5}$ concentrations in these cities were high in January and December ($118 \mu\text{g}/\text{m}^3$ and $101 \mu\text{g}/\text{m}^3$, respectively), with the lowest value observed in July ($34 \mu\text{g}/\text{m}^3$) (Figure 5). The reason for this result was that coal was burned for heating in the winter during this period, thereby inducing serious $PM_{2.5}$ pollution. After this period, the weather gradually warmed and heating with coal decreased, causing $PM_{2.5}$ concentrations to decrease in a fluctuating manner over time, resulting in gradually improving air quality. Air quality became better from March to October. $PM_{2.5}$ pollution started to become serious after November, and the cycle of $PM_{2.5}$ variation began again. The intra-month changes were largest between January and February, and between November and December, and the data distribution was dispersed (Table 1).

The $PM_{2.5}$ concentration in 2017 reached the highest value compared to the other years within the 2015 to 2021 timeframe (Figure 2), which can fully reflect the variation characteristics of $PM_{2.5}$ pollution in the study area. Taking 2017 as an example, we can see that the temporal variation characteristics of $PM_{2.5}$ concentrations were similar for the four cities. High $PM_{2.5}$ values were generally observed in January and February, with the maximum $PM_{2.5}$ concentrations occurring in early January (Linfen: $537 \mu\text{g}/\text{m}^3$, Yuncheng: $596 \mu\text{g}/\text{m}^3$, Weinan: $438 \mu\text{g}/\text{m}^3$, and Sanmenxia: $334 \mu\text{g}/\text{m}^3$). Another time period of high $PM_{2.5}$ concentrations occurred in November and December, when $PM_{2.5}$ pollution processes occurred in the first ten days, the middle ten days, and the last ten days of each month (Figure 6).

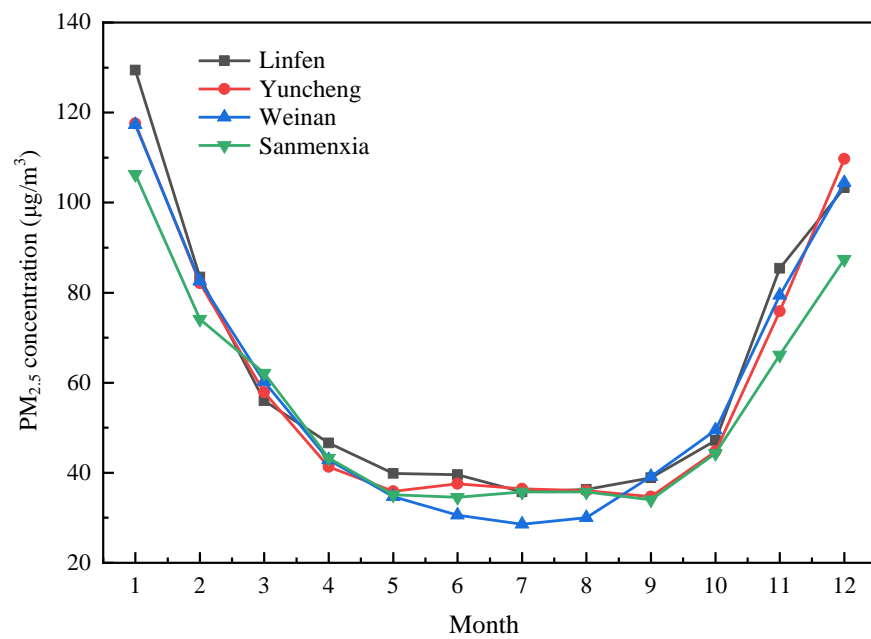


Figure 4. Monthly average PM_{2.5} concentrations for four cities in the Yellow River Golden Triangle Demonstration Area, China, from 2015 to 2021.

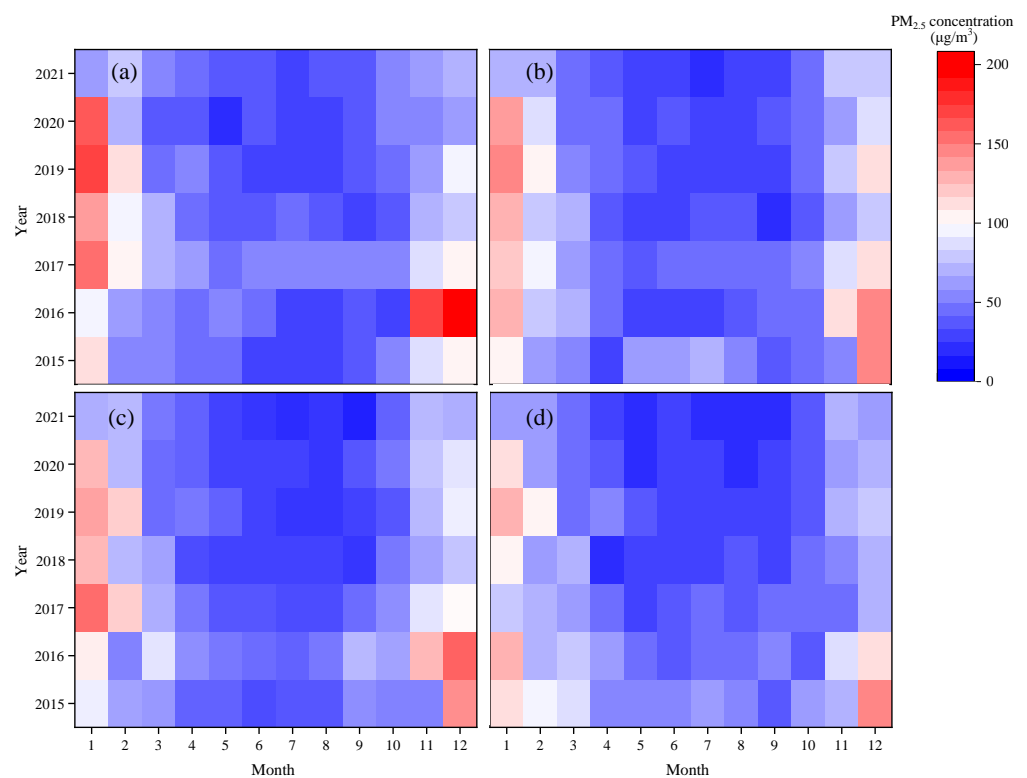


Figure 5. Monthly PM_{2.5} concentrations for four cities in the Yellow River Golden Triangle Demonstration Area, China, from 2015 to 2021. (a) represents Linfen, (b) represents Yuncheng, (c) represents Weinan, and (d) represents Sanmenxia.

Table 1. Statistical characteristics of monthly average PM_{2.5} concentrations in the Yellow River Golden Triangle Demonstration Area, China, from 2015 to 2021 (unit: µg/m³). Mini represents Minimum, Max represents Maximum, and Mean represents Average.

Month	Linfen			Yuncheng			Weinan			Sanmenxia		
	Mini	Max	Mean	Min	Max	Mean	Mini	Max	Mean	Mini	Maxi	Mean
1	66	174	129	67	144	118	69	158	117	65	132	106
2	54	114	83	63	107	82	53	120	83	59	103	74
3	37	74	56	46	71	58	45	90	60	42	90	62
4	36	59	47	33	48	41	30	58	43	22	59	43
5	24	54	40	28	64	36	25	49	35	23	58	35
6	30	58	40	28	65	38	23	43	31	25	54	35
7	28	54	36	22	68	36	18	39	29	18	60	36
8	26	57	36	26	56	36	21	48	30	22	54	36
9	31	57	39	21	44	35	16	71	39	20	54	34
10	30	57	47	39	52	45	37	64	49	35	60	44
11	57	173	85	57	111	76	53	128	79	49	88	66
12	63	206	103	77	148	110	68	160	104	61	142	87

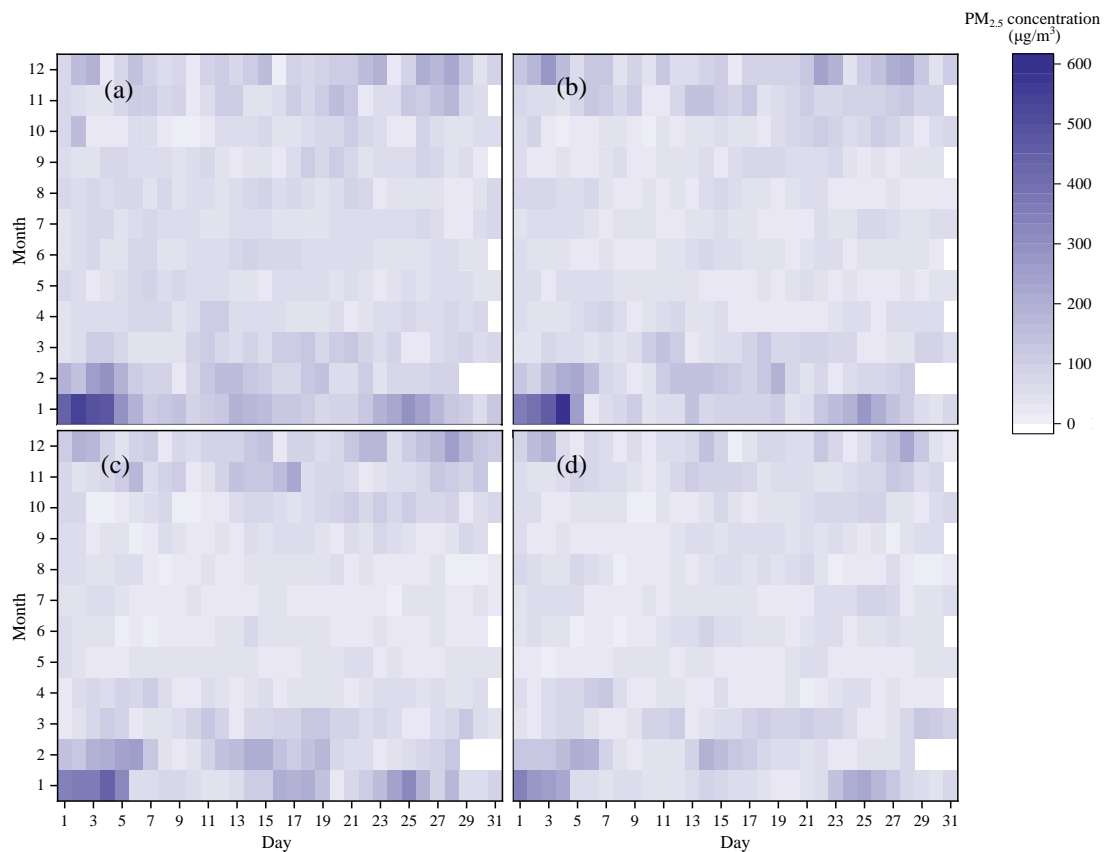


Figure 6. Temporal variation of PM_{2.5} concentrations in four cities in the Yellow River Golden Triangle Demonstration Area, China, in 2017. (a) represents Linfen, (b) represents Yuncheng, (c) represents Weinan, and (d) represents Sanmenxia.

3.2. Spatial Variation Characteristics of PM_{2.5} Concentrations in YRGTDA

The annual average PM_{2.5} concentrations data of 2000–2018 were obtained from the Atmospheric Composition Analysis Group of Dalhousie University. The spatial variation characteristics of PM_{2.5} concentrations in YRGTDA are shown in Figure 7. The spatial distribution of PM_{2.5} concentrations in YRGTDA was generally observed to be high in the central region and low in the northern and southern regions. The highest values of the minimum, average, and maximum PM_{2.5} concentrations were mainly located in the plain

areas of Linfen and Yuncheng (Figure 7a–c). The spatial distribution of the minimum $PM_{2.5}$ concentrations showed a decreasing trend from the plain areas of Linfen and Yuncheng to the northeast and southwest, respectively, and decreased more in the northeast direction than in the southwest direction. The distribution of the high values of average $PM_{2.5}$ concentrations was largely related to the significant inversion effect caused by the special local basin topography that made it difficult to spread air pollution. The low values of average $PM_{2.5}$ concentrations were located at the northwestern part of Linfen that generally had higher altitude, lower population, and less development of industry than the other cities. Overall, the distribution of the maximum $PM_{2.5}$ concentrations showed a decreasing trend from northeast to southwest. The spatial distribution of the annual variation of $PM_{2.5}$ concentrations in YRGTDA varied for different areas. The northeast region showed an increasing trend, the central region showed a small change, and the southwest region showed a decreasing trend (Figure 7d).

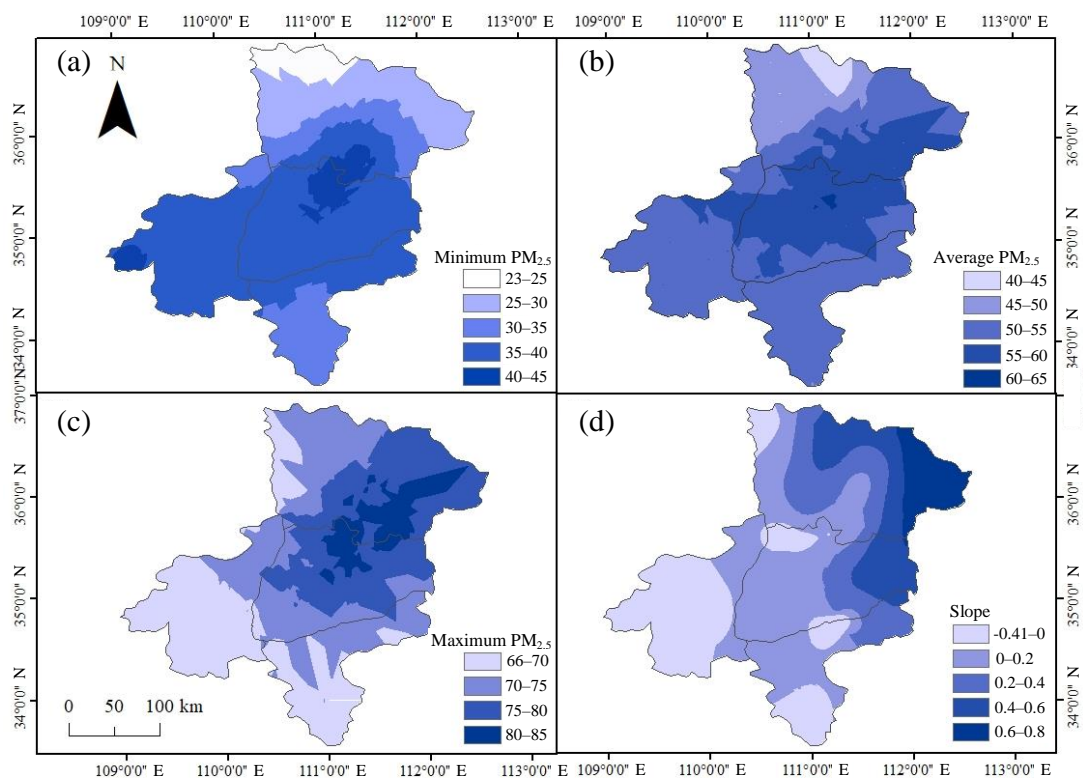


Figure 7. Spatial distribution of the minimum, average, maximum, and changes of annual average $PM_{2.5}$ concentrations of 2000–2018 in the Yellow River Golden Triangle Demonstration Area, China. (a) represents Linfen, (b) represents Yuncheng, (c) represents Weinan, and (d) represents Sanmenxia.

Spatial autocorrelation analysis was used to test the spatial autocorrelation of $PM_{2.5}$ concentrations in the counties of YRGTDA. The hotspot analysis of the $PM_{2.5}$ concentrations in the study area showed a cyclical variation pattern. From January to April, the coldspots were mainly located in the northwest, west, and south, while the hotspots were mainly located in the northeast. In general, the hotspot areas were mainly located in the plain of Linfen and the coldspot areas were mainly located in the mountainous area. This distribution corresponded to the distribution of population and coal-heated areas. The hotspot area expanded from May to August, and the coldspot area shifted to the west. In August, there was an obvious distribution pattern of hotspots in the northeast and coldspots in the southwest. The structure of industry and energy had an important influence on the regional $PM_{2.5}$ concentrations. From September to December, the hotspots gradually shifted to the south and the coldspots gradually shifted to the north (Figure 8).

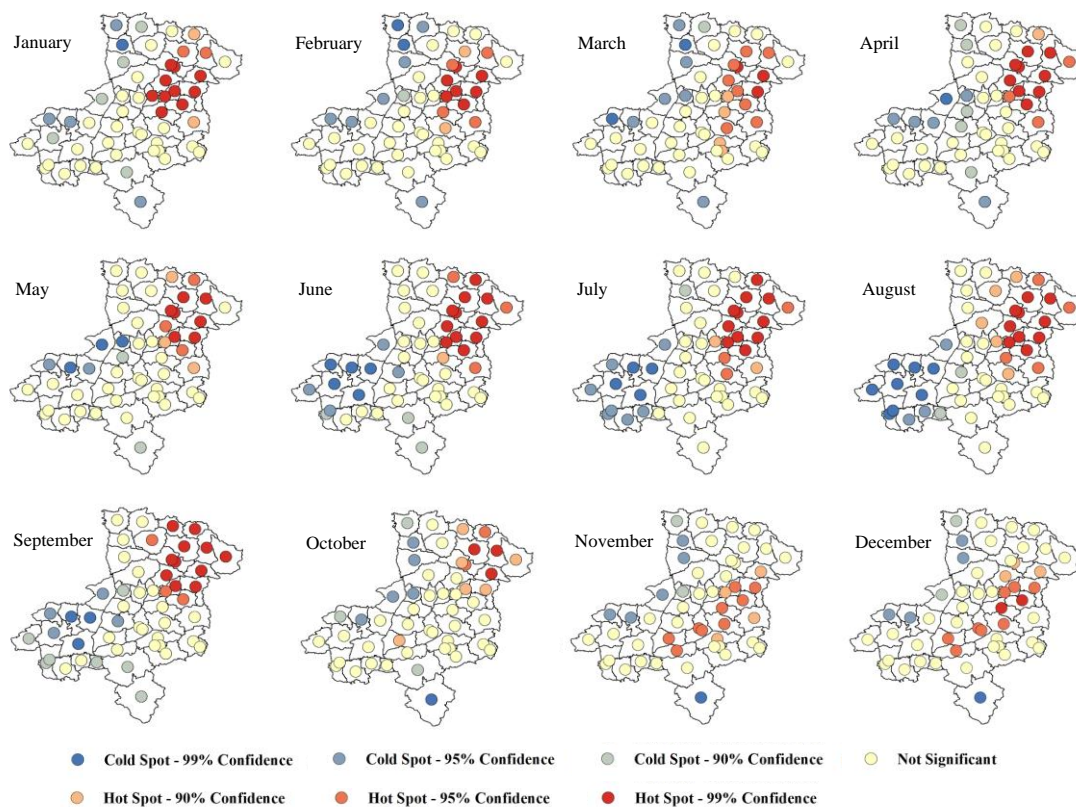


Figure 8. Hotspot analysis of $PM_{2.5}$ concentrations in the Yellow River Golden Triangle Demonstration Area, China, from January to December in 2017.

The warm and cold colors indicate the spatial clustering of the high or low values of $PM_{2.5}$ concentrations. The warm colors represent the tight clustering of high values of $PM_{2.5}$ concentrations (hotspots). The cold colors represent the tight clustering of low values of $PM_{2.5}$ concentrations (coldspots). The regions with statistically significant clustering patterns indicate that the $PM_{2.5}$ concentrations are spatially correlated.

3.3. Analysis of $PM_{2.5}$ Pollution Processes in YRGTDA

3.3.1. Annual Variation of $PM_{2.5}$ Pollution Classes

The variation of $PM_{2.5}$ pollution classes from 2015 to 2021 was analyzed for the four cities in YRGTDA according to China's Ambient Air Quality Standards (B3095-2012). The results showed that there were different numbers of pollution days in this region every year (Figure 9). The number of days in the various pollution classes followed the order of Good > Excellent > Light pollution > Moderate pollution > Heavy pollution > Severe pollution, and the number days in the Good and Excellent classes accounted for more than 70% of the total pollution days. The variation characteristics of the pollution classes were similar for the four cities in YRGTDA. Taking Yuncheng as an example, we can see that the number of days in the Excellent class ranged from 73 to 188 days (mean of 137 days), the number of days in the Good class ranged from 110 to 203 days (mean of 143 days), the number of days in the Light pollution class ranged from 35 to 65 days (mean of 46 days), the number of days in the Moderate pollution class ranged from nine to 29 days (mean of 19 days), the number of days in the Heavy pollution class ranged from four to 22 days (mean of 16 days), and the number of days in the Severe pollution class ranged from 0 to seven days (average of four days). According to the variation of annual $PM_{2.5}$ concentrations, the number of days in the Excellent class in YRGTDA were increasing, while the number days in the other five classes were decreasing.

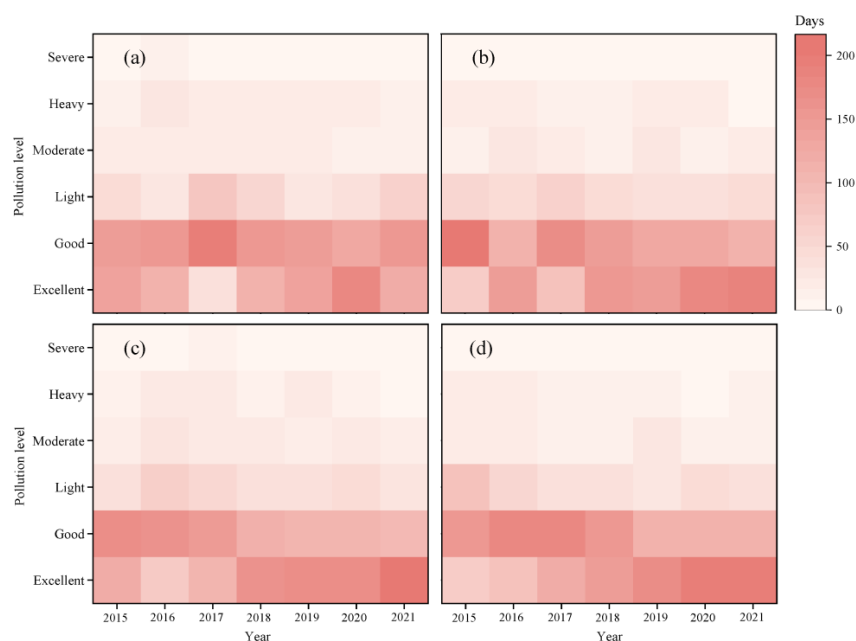


Figure 9. Variation characteristics of the number of annual days of different classes of PM_{2.5} pollution in the Yellow River Golden Triangle Demonstration Area, China. (a) represents Linfen, (b) represents Yuncheng, (c) represents Weinan, and (d) represents Sanmenxia.

3.3.2. Monthly and Seasonal Variation Characteristics of PM_{2.5} Pollution Levels

According to the Technical Regulation on Ambient Air Quality Index (on trial), the PM_{2.5} concentrations were divided into six classes. The monthly variation of PM_{2.5} pollution was similar for the four cities in YRGTD, showing a U-shaped variation (Figure 10). The order of number of days for PM_{2.5} pollution classes at the monthly scale followed the order of: Good > Excellent > Light pollution > Moderate pollution > Heavy pollution > Severe pollution, in which the number of days in the Good and Excellent classes accounted for more than 70% of the year. For Linfen, the maximum number of days for the Excellent class occurred in July (18.7 days) and the minimum number of Excellent days occurred in January (2.7 days). The maximum number of Good days occurred in April (21.0 days) and the minimum number of Good days occurred in January (5.0 days). The maximum days for the Light pollution class occurred in February (9.1 days) and the minimum number of Light pollution days occurred in July (0.6 days). The maximum number of days for the Moderate pollution class occurred in January (5.7 days) and the minimum number of Moderate pollution days occurred from June to September (0 days). The maximum number of days for the Heavy pollution class occurred in January (7.4 days) and the minimum number of Heavy pollution days occurred from May to September (0 days). The maximum number of days for the Severe pollution class occurred in January (3.3 days) and the minimum number of Severe pollution days occurred from March to October (0 days).

In YRGTD, the variation characteristics of the number of days in each pollution class of seasonal PM_{2.5} concentrations showed that the number of days for the Heavy pollution class were mostly in winter, the highest number of days for the Good class occurred mostly in spring and autumn, and the highest number of days for the Excellent class occurred mostly in summer (Figure 11). There was an obvious cyclical fluctuation for the variation of PM_{2.5} pollution levels between seasons. From 2015 to 2021, the number of days of Heavy and Severe pollution in winter showed a decreasing trend, while the number days in the Excellent class was increasing in summer. For Linfen, the number of days for the Excellent class followed the order of summer (51 days) > autumn (30 days) > spring (26 days) > winter (12 days). For the Good class, the order was spring (54 days) > autumn (41 days) > summer (38 days) > winter (21 days), and for the Light to Severe pollution classes, the order was winter > autumn > spring > summer.

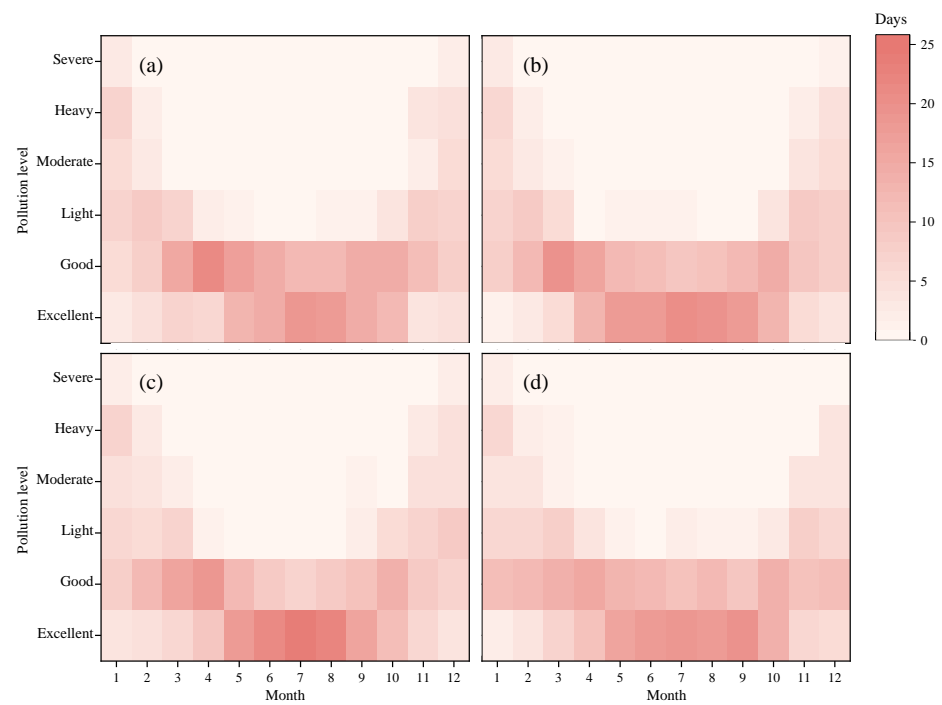


Figure 10. Variation characteristics of monthly average $PM_{2.5}$ concentration classes in the Yellow River Golden Triangle Demonstration Area, China. (a) represents Linfen, (b) represents Yuncheng, (c) represents Weinan, and (d) represents Sanmenxia.

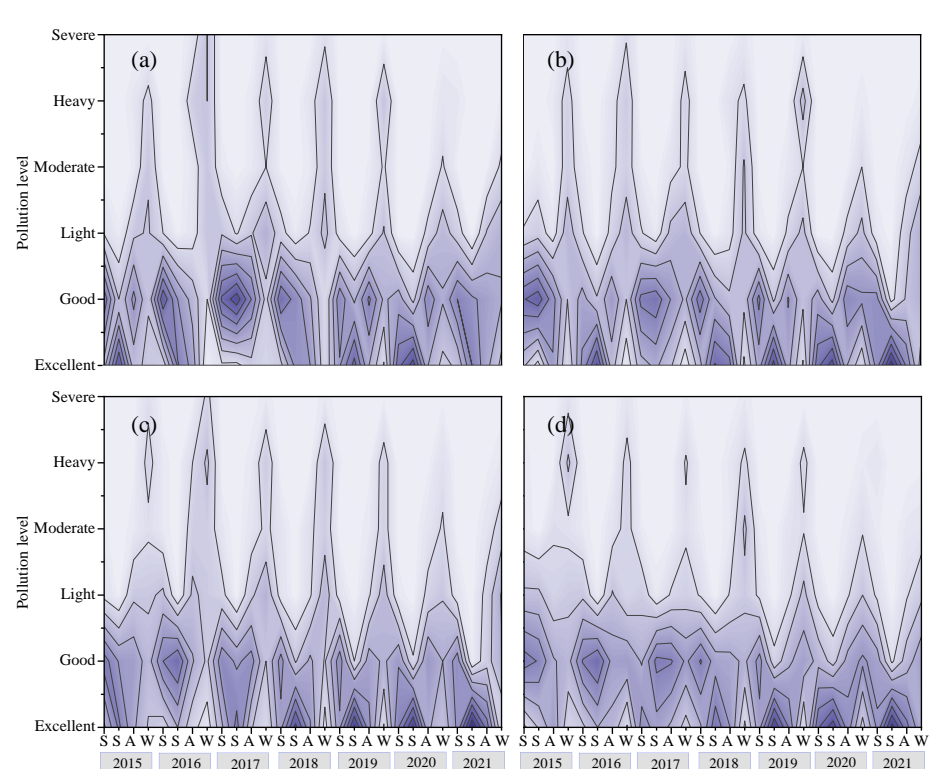


Figure 11. Variation in the number of days in various pollution classes for seasonal average $PM_{2.5}$ concentrations in the Yellow River Golden Triangle Demonstration Area, China. First S is spring, second S is summer, A is autumn, W is winter. (a) represents Linfen, (b) represents Yuncheng, (c) represents Weinan, and (d) represents Sanmenxia.

4. Discussion

This study focused on the spatiotemporal variation of $PM_{2.5}$ concentrations at annual, seasonal, and monthly scales in YRGTD. The $PM_{2.5}$ concentrations showed an increasing trend from 2000 to 2011 in YRGTD and a decreasing trend from 2011 to 2021, with 2011 being an important inflection year. The $PM_{2.5}$ concentrations decreased during 2011–2021, mainly due to the adoption of a series of measures related to national ecological civilization construction, ecological compensation pilot, pollution census, environmental protection policies, national industrial restructuring, energy efficiency improvement, etc. These measures suppressed the emission of particulate matter to a certain extent. Xiao et al. (2017) found the annual average $PM_{2.5}$ concentrations of Yangtze River Delta varied greatly in spatial distribution [25]. Guo et al. (2017) and Jiang et al. (2021) analyzed the spatial distribution of annual average $PM_{2.5}$ concentrations [7,20]. Wang et al. (2023) conducted a study of $PM_{2.5}$ concentrations in the Fenwei Plain [8]. The results in this study are consistent with these above studies, i.e., high $PM_{2.5}$ concentrations occurred in Linfen and Yuncheng city. In this study, high values of $PM_{2.5}$ concentrations generally occurred in winter and low values occurred in summer. Chen et al. (2019) obtained the similar results when analyzing the seasonal variation characteristics of $PM_{2.5}$ concentrations at a national scale [3]. Lin et al. (2015) estimated the ground-level $PM_{2.5}$ using MODIS-observed AOD and found the spatial distribution characteristics of seasonal $PM_{2.5}$ were consistent with the results in this study [24]. At the monthly scale, high $PM_{2.5}$ values occurred in January and December and low values occurred in June. The studies of Zhang et al. (2022) and Dai et al. (2023) showed low values of $PM_{2.5}$ concentrations generally occurred in June and July, while high values occurred in January and December. The results in this study were consistent with these previous studies [4,5]. In this study, only the spatiotemporal variations of $PM_{2.5}$ concentrations were analyzed. The effects of meteorological and natural conditions, and the interactive coupling between the influencing factors, were not considered [34,35]. In the future, spatial autocorrelation and geostatistical methods will be used to study the spatiotemporal variation characteristics of $PM_{2.5}$ concentration. These future studies will be helpful in providing an important reference for the implementation of effective environmental pollution prevention and control in YRGTD.

$PM_{2.5}$ pollution levels were analyzed based on the spatiotemporal characteristics of $PM_{2.5}$ concentrations in YRGTD. The results showed that there were different degrees of pollution days in YRGTD every year during the study period. Days classified as Good were most often observed, while days classified as Severe pollution were least often observed. In winter, days classified as Heavy pollution were most often observed, and the number of days with this classification decreased with time. In the summer, days classified as Excellent were most often observed, and the number of days with this classification increased with time. During the process of atmospheric pollution, the frequency, duration, and peak concentration of $PM_{2.5}$ can directly affect the occurrence probability of heavy pollution events and pollution levels. In this study, we did not conduct an analysis of duration and peak concentration of $PM_{2.5}$ pollution. Further research will be needed to study the characteristics of the pollution process in this region in order to provide the necessary research basis for clarifying the characteristics, classification, and occurrence mechanism of the heavy pollution process in this region.

There are many heavy chemical enterprises in YRGTD. This region is a concentrated distribution area for coal, iron, steel, and other heavy chemical enterprises. For a long time, the high $PM_{2.5}$ concentrations in this region have been due to industrial emissions. In addition, rapid urbanization here has led to a migration of population to large and medium-sized cities that has intensified the emission of related pollutants. $PM_{2.5}$ pollution is influenced by both natural and socioeconomic factors. Many studies have been conducted to analyze the relationship between variations in $PM_{2.5}$ concentrations and factors such as urbanization level, industrial structure, industrial development level, population, other socioeconomic factors, etc. [3,36]. Future studies will focus on analyzing the relationship between $PM_{2.5}$ and socio-economic factors in YRGTD. Then, targeted prevention and control countermeasures can be developed. The results of this study and future studies will be helpful in providing

decision support for adjusting and optimizing the industrial structure, energy consumption structure, and transportation structure, and for mitigating air pollution, reducing the risk of population exposure to pollution, and protecting public health.

5. Conclusions

In this study, the spatiotemporal variation characteristics of PM_{2.5} concentrations and pollution levels in YRGTDA were analyzed. Results showed that: (1) at different time scales, the annual average PM_{2.5} concentrations showed an increasing trend from 2000 to 2011 and a decreasing trend from 2011 to 2021 in the study area. The PM_{2.5} concentrations reached their highest values in 2011. After 10 years of environmental governance and ecological protection, the PM_{2.5} concentrations observed in 2021 had recovered to the level observed in 2000. The PM_{2.5} concentrations were high and varied greatly in winter, while the concentrations were low and varied slightly in summer. Spring and autumn were transitional periods for PM_{2.5} concentrations. PM_{2.5} concentrations showed a U-shaped variation pattern from January to December each year, with the highest PM_{2.5} concentrations occurring in January and December and the lowest PM_{2.5} concentrations occurring in July. (2) PM_{2.5} pollution in YRGTDA exhibited high spatial heterogeneity, with distribution characteristics of high values in the central part of the YRGTDA and low values in the northern and southern parts. The highest values of the minimum, maximum, and average PM_{2.5} concentrations were mainly located in the plains of Linfen and Yuncheng in the north part of the study area. The spatial distribution of the annual variation of PM_{2.5} concentrations varied significantly across the study area. There was an increasing trend of PM_{2.5} concentrations in the northeastern part of the study area, a gentle change in the central part, and a decreasing trend in the southwestern part. (3) The hotspot analysis of the PM_{2.5} concentrations in the study area showed a cyclical variation pattern. From January to April, the coldspots were mainly located in the northwest, west, and south parts of the study area, while the hotspots were mainly located in the northeast. From May to August, the area of hotspots expanded and the coldspots shifted to the west. In August, there was an obvious distribution pattern of hotspots in the northeast and coldspots in the southwest. From September to December, the hotspots gradually shifted to the south and the coldspots gradually shifted to the north. (4) There were different classes of pollution in YRGTDA every year. The number of days in the six pollution classes followed the order of Good > Excellent > Light pollution > Moderate pollution > Heavy pollution > Severe pollution. The number of days classified as Good and Excellent accounted for more than 70% of the year. The number of days classified as Excellent in this region increased over time, while the number of days of other five pollution classes decreased over time. During 2015–2021, the days classified as Heavy pollution occurred mostly in winter (with a decreasing trend), the days classified as Good occurred mostly in spring and autumn, and the days classified as Excellent occurred mostly in summer (with an increasing trend).

Author Contributions: Conceptualization, N.J., L.H. and D.Z.; methodology, N.J. and M.Q.; software, N.J. and H.J.; writing—original draft preparation, N.J. and C.W.; writing—review and editing, X.L. and Y.L. All authors have read and agreed to the published version of the manuscript.

Funding: This work was funded by the Science and Technology Innovation 2030—“New Generation Artificial Intelligence” Major Project (2021ZD0113605), the Science and Technology Plan of Inner Mongolia Autonomous Region Project (Grant No. 2022YFSJ0039), the Key Research and Technology Development Projects of Anhui Province (Grant No. 202004a06020045), and the Natural Science Foundation of China (No.41705095).

Institutional Review Board Statement: Not applicable.

Informed Consent Statement: Not applicable.

Data Availability Statement: All data that support the findings of this study are available from the corresponding author upon reasonable request.

Conflicts of Interest: The authors declare no conflict of interest.

References

1. Al-Qaness, M.A.A.; Fan, H.; Ewees, A.A.; Yousri, D.; Elaziz, M.A. Improved ANFIS model for forecasting Wuhan City Air Quality and analysis COVID-19 lockdown impacts on air quality. *Environ. Res.* **2021**, *194*, 110607. [[CrossRef](#)] [[PubMed](#)]
2. Meij, A.D.; Thunis, P.; Bessagnet, B.; Cuvelier, C. The sensitivity of the CHIMERE model to emissions reduction scenarios on air quality in Northern Italy. *Atmos. Environ.* **2009**, *43*, 1897–1907. [[CrossRef](#)]
3. Chen, Z.Y.; Chen, D.L.; Xie, X.M.; Xie, X.M.; Cai, J.; Zhuang, Y.; Cheng, N.L.; He, B.; Gao, B.B. Spatial self-aggregation effects and national division of city-level PM_{2.5} concentrations in China based on spatio-temporal clustering. *J. Clean. Prod.* **2019**, *207*, 875–881. [[CrossRef](#)]
4. Zhang, Y.; Zhai, S.W.; Huang, J.F.; Li, X.L.; Wang, W.; Zhang, T.; Yin, F.; Ma, Y. Estimating high-resolution PM_{2.5} concentration in the Sichuan Basin using a random forest model with data-driven spatial autocorrelation terms. *J. Clean. Prod.* **2022**, *380*, 134890. [[CrossRef](#)]
5. Dai, M.; Liu, A.; Sheng, Y.; Xian, Y.; Wang, H.; Wang, C. Analysis of PM_{2.5} Characteristics in Yancheng from 2017 to 2021 Based on Kolmogorov–Zurbenko Filter and PSCF Model. *Atmosphere* **2023**, *14*, 317. [[CrossRef](#)]
6. Guo, S.; Tao, X.; Liang, L. Exploring Natural and Anthropogenic Drivers of PM_{2.5} Concentrations Based on Random Forest Model: Beijing–Tianjin–Hebei Urban Agglomeration, China. *Atmosphere* **2023**, *14*, 381. [[CrossRef](#)]
7. Jiang, T.T.; Chen, B.; Nie, Z.; Ren, Z.H.; Xu, B.; Tang, S.H. Estimation of hourly full-coverage PM_{2.5} concentrations at 1-km resolution in China using a two-stage random forest model. *Atmos. Res.* **2021**, *248*, 105146. [[CrossRef](#)]
8. Wang, Y.; Cao, L.; Zhang, T.; Kong, H. Simulations of Summertime Ozone and PM_{2.5} Pollution in Fenwei Plain (FWP) Using the WRF-Chem Model. *Atmosphere* **2023**, *14*, 292. [[CrossRef](#)]
9. Kelly, J.T.; Jang, C.; Timin, B.; Di, Q.; Schwartz, J.; Liu, Y.; Donkelaar, A.V.; Martin, R.V.; Berrocal, V.; Bell, M.L. Examining PM_{2.5} concentrations and exposure using multiple models. *Environ. Res.* **2021**, *196*, 110432. [[CrossRef](#)]
10. Zhang, T.; Su, Y.; Deboz, J.; Noble, M.; Munoz, A.; Xu, X. Continuous Measurements and Source Apportionment of Ambient PM_{2.5}-Bound Elements in Windsor, Canada. *Atmosphere* **2023**, *14*, 374. [[CrossRef](#)]
11. Chen, J.D.; Wang, B.; Huang, S.; Song, M.L. The influence of increased population density in China on air pollution. *Sci. Total Environ.* **2020**, *735*, 139456. [[CrossRef](#)] [[PubMed](#)]
12. Yitshak-Sade, M.; Bobb, J.F.; Schwartz, J.D.; Kloog, I.; Zanobetti, A. The association between short and long-term exposure to PM_{2.5} and temperature and hospital admissions in New England and the synergistic effect of the short-term exposures. *Sci. Total Environ.* **2018**, *639*, 868–875. [[CrossRef](#)] [[PubMed](#)]
13. Lu, H.; Xie, M.; Liu, B.J.; Liu, X.R.; Feng, J.L.; Yang, F.Y.; Zhao, X.L.; You, T.; Wu, Z.; Gao, Y.H. Impact of atmospheric thermodynamic structures and aerosol radiation feedback on winter regional persistent heavy particulate pollution in the Sichuan-Chongqing region, China. *Sci. Total Environ.* **2022**, *842*, 156575. [[CrossRef](#)] [[PubMed](#)]
14. Yahya, K.; Zhang, Y.; Vukovich, J.M. Real-time air quality forecasting over the southeastern United States using WRF/Chem-MADRID: Multiple-year assessment and sensitivity studies. *Atmos. Environ.* **2014**, *92*, 318–338. [[CrossRef](#)]
15. Du, J.B.; Qiao, F.X.; Yu, L. Temporal characteristics and forecasting of PM_{2.5} concentration based on historical data in Houston, USA, Resources. *Conserv. Recycl.* **2019**, *147*, 145–156. [[CrossRef](#)]
16. Montes, C.; Sapkota, T.; Singh, B. Seasonal patterns in rice and wheat residue burning and surface PM_{2.5} concentration in northern India. *Atmos. Environ.* **2022**, *13*, 100154. [[CrossRef](#)]
17. Zhao, S.P.; Yu, Y.; Qin, D.H.; Yin, D.Y.; Dong, L.X.; He, J.J. Analyses of regional pollution and transportation of PM_{2.5} and ozone in the city clusters of Sichuan Basin, China. *Atmos. Pollut. Res.* **2019**, *10*, 374–385. [[CrossRef](#)]
18. Gonçalves, K.D.S.; Winkler, M.S.; Benchimol-Barbosa, P.R.; Hoogh, K.D.; Artaxo, P.E.; Hacon, S.D.S.; Schindler, C.; Künzli, N. Development of non-linear models predicting daily fine particle concentrations using aerosol optical depth retrievals and ground-based measurements at a municipality in the Brazilian Amazon region. *Atmos. Environ.* **2018**, *184*, 156–165. [[CrossRef](#)]
19. Guzmán, P.; Tarín-Carrasco, P.; Morales-Suárez-Varela, M.; Jiménez-Guerrero, P. Effects of air pollution on dementia over Europe for present and future climate change scenarios. *Environ. Res.* **2022**, *204*, 112012. [[CrossRef](#)]
20. Guo, H.; Cheng, T.H.; Gu, X.F.; Wang, Y.; Chen, H.; Bao, F.W.; Shi, S.Y.; Xu, B.R.; Wang, W.N.; Zuo, X.; et al. Assessment of PM_{2.5} concentrations and exposure throughout China using ground observations. *Sci. Total Environ.* **2017**, *601*, 1024–1030. [[CrossRef](#)]
21. Jurado, X.; Reiminger, N.; Maurer, L.; Vazquez, J.; Wemmert, C. On the Correlations between Particulate Matter: Comparison between Annual/Monthly Concentrations and PM₁₀/PM_{2.5}. *Atmosphere* **2023**, *14*, 385. [[CrossRef](#)]
22. Xu, R.; Wang, D.; Li, J.; Wan, H.; Shen, S.; Guo, X. A Hybrid Deep Learning Model for Air Quality Prediction Based on the Time–Frequency Domain Relationship. *Atmosphere* **2023**, *14*, 405. [[CrossRef](#)]
23. Zhai, S.W.; Zhang, Y.; Huang, J.F.; Li, X.L.; Wang, W.; Zhang, T.; Yin, F.; Ma, Y. Exploring the detailed spatiotemporal characteristics of PM_{2.5}: Generating a full-coverage and hourly PM_{2.5} dataset in the Sichuan Basin, China. *Chemosphere* **2023**, *310*, 136786. [[CrossRef](#)]
24. Liu, C.Q.; Li, Y.; Yuan, Z.B.; Lau, A.K.H.; Li, C.C.; Fung, J.C.H. Using satellite remote sensing data to estimate the high-resolution distribution of ground-level PM_{2.5}. *Remote Sens. Environ.* **2015**, *156*, 117–128.
25. Xiao, Q.Y.; Wang, Y.J.; Chang, H.H.; Meng, X.; Geng, G.N.; Lyapustin, A.; Liu, Y. Full-coverage high-resolution daily PM_{2.5} estimation using MAIAC AOD in the Yangtze River Delta of China. *Remote Sens. Environ.* **2017**, *199*, 437–446. [[CrossRef](#)]
26. Bi, J.Z.; Belle, J.H.; Wang, Y.J.; Lyapustin, A.I.; Wildani, A.; Liu, Y. Impacts of snow and cloud covers on satellite-derived PM_{2.5} levels. *Remote Sens. Environ.* **2019**, *221*, 665–674. [[CrossRef](#)] [[PubMed](#)]

27. Hoogh, K.D.; Héritier, H.; Stafoggia, M.; Künzli, N.; Kloog, I. Modelling daily PM_{2.5} concentrations at high spatio-temporal resolution across Switzerland. *Environ. Pollut.* **2018**, *233*, 1147–1154. [[CrossRef](#)]
28. James, T.K.; Shannon, N.K.; Kirk, R.B.; Amara, L.H.; Havalala, O.T.P.; Benjamin, N.M.; Jesse, O.B.; Barron, H.H.; Norman, C.P.; Heather, S.; et al. Assessing PM_{2.5} model performance for the conterminous U.S. with comparison to model performance statistics from 2007–2015. *Atmos. Environ.* **2019**, *214*, 116872.
29. Van Donkelaar, A.; Martin, R.V.; Brauer, M.; Hsu, N.C.; Kahn, R.A.; Levy, R.C.; Lyapustin, A.; Sayer, A.M.; Winker, D.M. Global estimates of fine particulate matter using a combined geophysical-statistical method with information from satellites, models, and monitors. *Environ. Sci. Technol.* **2016**, *50*, 3762–3772. [[CrossRef](#)]
30. Malik, S.; Pal, S.C.; Sattar, A.; Singh, S.K.; Mohammad, P. Trend of extreme rainfall events using suitable global circulation model to combat the water logging condition in kolkata metropolitan area. *Urban Clim.* **2020**, *32*, 100599. [[CrossRef](#)]
31. Zhang, X.; Gong, Z. Spatiotemporal characteristics of urban air quality in China and geographic detection of their determinants. *J. Geogr. Sci.* **2018**, *28*, 563–578. [[CrossRef](#)]
32. Askariyeh, M.H.; Venugopal, M.; Khreis, H.; Birt, A.; Zietsman, J. Near-Road Traffic-Related Air Pollution: Resuspended PM_{2.5} from Highways and Arterials. *Int. J. Environ. Res. Public Health* **2020**, *17*, 2851. [[CrossRef](#)] [[PubMed](#)]
33. Fang, C.; Wang, L.; Li, Z.; Wang, J. Spatial Characteristics and Regional Transmission Analysis of PM_{2.5} Pollution in Northeast China, 2016–2020. *Int. J. Environ. Res. Public Health* **2021**, *18*, 12483. [[CrossRef](#)] [[PubMed](#)]
34. Li, C.; Li, Z.Z.; Zhang, F.M.; Lu, Y.Y.; Duan, C.F.; Xu, Y. Seasonal dynamics of carbon dioxide and water fluxes in a rice-wheat rotation system in the Yangtze-Huaihe region of China. *Agric. Water Manag.* **2023**, *275*, 107992. [[CrossRef](#)]
35. Li, Z.; Wu, Y.; Wang, R.; Liu, B.; Qian, Z.; Li, C. Assessment of climatic impact on vegetation spring phenology in northern China. *Atmosphere* **2023**, *14*, 117. [[CrossRef](#)]
36. Pisoni, E.; Dominguez-Torreiro, M.; Thunis, P. Inequality in exposure to air pollutants: A new perspective. *Environ. Res.* **2022**, *212*, 113358. [[CrossRef](#)]

Disclaimer/Publisher's Note: The statements, opinions and data contained in all publications are solely those of the individual author(s) and contributor(s) and not of MDPI and/or the editor(s). MDPI and/or the editor(s) disclaim responsibility for any injury to people or property resulting from any ideas, methods, instructions or products referred to in the content.